

Leptonic decays of D_s and B^+ mesons in supersymmetric standard model with R -parity violating interactions

Yumiko Aida¹⁾, Eri Asakawa²⁾, Gi-Chol Cho²⁾, Hikaru Matsuo¹⁾

¹⁾*Graduate School of Humanities and Sciences, Ochanomizu University, Tokyo, 112-8610, Japan*

²⁾*Department of Physics, Ochanomizu University, Tokyo 112-8610, Japan*

Abstract

We investigate leptonic decays $D_s \rightarrow \tau \nu_\tau$ and $B^+ \rightarrow \tau \nu_\tau$ in R -parity violating (RPV) supersymmetric standard model. Taking account of interference between the s -channel slepton exchange and the t -channel squark exchange diagrams, we find that the supersymmetric contributions are cancelled between two diagrams so that the RPV couplings could be sizable under the experimental bounds. Constraints on the relative sign between the RPV couplings in s - and t -channel diagrams are also discussed.

1 Introduction

Supersymmetric extension of the standard model (SM) [1] is a leading candidate of physics beyond the SM. However, since no experimental evidence of supersymmetry (SUSY) has not been found yet, discovery of supersymmetric particles at energy frontier experiments such as LHC is one of the important tasks of particle physics.

The most general gauge invariant and renormalizable superpotential in the supersymmetric SM contains baryon (B) and lepton (L) number violating interactions which may lead to unwanted fast proton decay or sizable lepton number violating processes. Such interactions can be forbidden by introducing so called R -parity which is defined as $R = (-1)^{3B+L+2S}$, where S denotes the spin quantum number. Owing to the R -parity, in addition to the suppression of B - and L -violating processes, the lightest supersymmetric particle (LSP) becomes stable, and it could be a candidate of dark matter. On the other hand, some of R -parity violating (RPV) interactions may play phenomenologically attractive role. For example, the R -parity and L -violating interactions may explain tiny neutrino mass without introducing the right-handed neutrinos [2]. Also, a possibility of gravitino dark matter due to the R -parity violating interactions has been discussed in ref. [3].

In this article, we study contribution of the RPV interactions to the leptonic decays of D_s and B^+ mesons. It is known that the experimental data of the leptonic decays of D_s and B^+ mesons slightly deviate from the SM expectations. Comparison of the experimental results of leptonic decay of D_s meson is often presented in terms of the decay constant f_{D_s} . The recent measurement of the leptonic decay of D_s meson by CLEO [4] is given by

$$f_{D_s} = 259.0 \pm 6.2 \pm 3.0 = 259.0 \pm 6.9 \text{ [MeV]}, \quad (1)$$

while the most precise calculation of f_{D_s} by HPQCD and UKQCD [5] is given as

$$f_{D_s} = 241 \pm 3 \text{ [MeV]}. \quad (2)$$

The discrepancy between (1) and (2) is about 2.4σ . The recent review of the experimental data and theoretical estimations on the decay constant f_{D_s} can be found in refs. [6].

For the leptonic decay $B^+ \rightarrow \tau \nu_\tau$, the experimental data of the branching ratio have been given by Belle and BABAR [7, 8]. The average of the data given by the UTfit collaboration [9] is

$$\text{BR}(B^+ \rightarrow \tau \nu_\tau)_{\text{exp}} = (1.73 \pm 0.34) \times 10^{-4}, \quad (3)$$

while the SM prediction is given by [9]

$$\text{BR}(B^+ \rightarrow \tau \nu_\tau)_{\text{SM}} = (0.84 \pm 0.11) \times 10^{-4}. \quad (4)$$

The difference between (3) and (4) is 2.5σ . The deviations in the leptonic decays in both D_s and B^+ may be statistical fluctuations. However, another interpretation of the deviations is that the deviations are caused by new physics beyond the SM. In the SM, these leptonic decays are dominated by the W -boson exchange at tree level¹. Therefore, a class of new physics models which lead to the leptonic decays at tree level could be candidates to explain the discrepancies, e.g., Two Higgs doublet model [11, 12, 13], leptoquark model [14, 15], and the R -parity violating supersymmetric SM [16, 17, 18, 19, 20, 21].

In the supersymmetric SM with RPV interactions, contributions to the leptonic decays of D_s and B^+ mesons are given by down-squark exchange in t -channel diagram, charged slepton exchange in s -channel diagram and charged Higgs boson exchange in s -channel diagram. In refs. [18, 19, 21], only the t -channel contribution was examined based on some scenarios or single coupling dominance hypothesis. The contribution of s -channel diagram in addition to the t -channel has been studied in refs. [16, 17, 20]. However, since works in refs. [16, 17] have been done before the first measurement of $B^+ \rightarrow \tau \nu_\tau$ in 2006 [7], bounds on the RPV couplings were not obtained from the experimental data of the B^+ decay. In ref. [20], constraints on the RPV couplings in s - and t -channel diagrams were investigated separately, and no interference effect between two diagrams was examined. In our study, we investigate the supersymmetric contributions to the leptonic decay of D_s and B^+ mesons taking account of the interference effects between the s - and t -channel diagrams. We also examine a diagram mediated by the charged Higgs boson in the s -channel. Taking account of the interference effects between the s - and t -channel diagrams, we show allowed region of the RPV couplings which explains the deviation between experimental data and the SM prediction. Note that the interference between two diagrams could be either constructive or destructive due to the relative sign of the RPV couplings in two diagrams. We find, therefore, that the experimental data constrains not only the size of RPV couplings but also the relative sign between the RPV couplings in s - and t -channel diagrams, which has not been examined in previous studies. The contribution of charged Higgs boson is found to be negligible in $D_s \rightarrow \tau \nu_\tau$, but sizable in $B^+ \rightarrow \tau \nu_\tau$. We discuss how the constraints on RPV couplings are affected by the charged Higgs contribution.

¹It has been pointed out that the radiative corrections are highly suppressed [10]

2 Set up

The R -parity violating interactions with trilinear couplings are described by the following superpotential

$$W_{\mathcal{R}} = \frac{1}{2}\lambda_{ijk}L_iL_jE_k + \lambda'_{ijk}L_iQ_jD_k + \frac{1}{2}\lambda''_{ijk}U_iD_jD_k, \quad (5)$$

where Q and L are $SU(2)_L$ doublet quark and lepton superfields, respectively. The up- and down-type singlet quark superfields are represented by U and D , while the lepton singlet superfield is E . The generation indices are labeled by i, j and k . The $SU(2)_L$ and $SU(3)_C$ gauge indices are suppressed. The coefficient λ_{ijk} is anti-symmetric for i and j , while λ''_{ijk} is anti-symmetric for j and k . For a comprehensive review of the R -parity violating supersymmetric SM, see, ref. [22]. Constraints on the RPV couplings λ_{ijk} , λ'_{ijk} and λ''_{ijk} from various processes have been studied in the literature [23, 24, 25, 26, 18]. Since the baryon number violating coupling λ''_{ijk} induces too fast proton decay, we take $\lambda''_{ijk} = 0$ in the following. Then, the leptonic decays of D_s and B^+ mesons occur through the t -channel exchange with a product of two λ' couplings while s -channel exchange is given by a product of λ and λ' .

Let us briefly summarize the leptonic decay of a pseudo scalar meson P which consists of the up and (anti-) down-type quarks u_a and \bar{d}_b , where a, b are generation indices of quarks. The decay width of $P \rightarrow l_i \nu_j$ is given as

$$\Gamma(P \rightarrow l_i \nu_j) = \frac{1}{8\pi} r_P^2 G_F^2 |V_{u_a d_b}^*|^2 f_P^2 m_{l_i}^2 m_P \left(1 - \frac{m_{l_i}^2}{m_P^2}\right)^2 \quad (6)$$

where G_F , $V_{u_a d_b}$, m_{l_i} and m_P are the Fermi constant, the Cabibbo-Kobayashi-Maskawa matrix element, the mass of a charged lepton l_i and the mass of a pseudo scalar meson P , respectively. The flavor indices of charged leptons and neutrinos are expressed by i and j , respectively. The decay constant is denoted by f_P . A parameter r_P is defined as,

$$r_P^2 \equiv \frac{|G_F V_{u_a d_b}^* + A_{ii}^P|^2}{G_F^2 |V_{u_a d_b}^*|^2} + \sum_{j(\neq i)} \frac{|A_{ij}^P|^2}{G_F^2 |V_{u_a d_b}^*|^2}, \quad (7)$$

where A_{ij}^P represents new physics contribution. Note that, in the second term of r.h.s. in (7), one should take a sum only for j (neutrinos), because that the neutrino flavor cannot be detected experimentally. If there is no new physics contribution, $r_P = 1$.

The interaction Lagrangian of the t -channel contribution to the decay width (6) can be obtained from the superpotential (5);

$$\mathcal{L} = \lambda'_{ijk} \left\{ -\overline{(l_L^c)_i} (u_L)_j (\tilde{d}_R)_k^* \right\} + \lambda'^*_{ijk} \left\{ (\tilde{d}_R)_k \overline{(d_L)_j} (\nu_L^c)_i \right\} + \text{h.c.} \quad (8)$$

Using the Fierz transformation, the effective Lagrangian which describes the t -channel squark exchange is given as

$$\mathcal{L}_{\text{eff}}^t = \frac{1}{8} \sum_{k=1}^3 \frac{\lambda'_{iak} \lambda_{jbk}^*}{m_{\tilde{d}_{Rk}}^2} \bar{\nu}_j \gamma^\mu (1 - \gamma_5) l_i \bar{d}_b \gamma_\mu (1 - \gamma_5) u_a. \quad (9)$$

For comparison, we show the effective Lagrangian for the W -boson exchange

$$\mathcal{L}_{\text{eff}}^{\text{SM}} = \frac{G_F}{\sqrt{2}} V_{u_a d_b}^* \bar{\nu}_i \gamma^\mu (1 - \gamma_5) l_i \bar{d}_b \gamma_\mu (1 - \gamma_5) u_a. \quad (10)$$

Using the decay constant f_P which is given by

$$\langle 0 | \bar{d}_b \gamma^\mu \gamma_5 u_a | P(q) \rangle = i f_P q^\mu, \quad (11)$$

we find the t -channel squark contribution to the decay $P(u_a \bar{d}_b) \rightarrow l_i \nu_j$ as

$$(A_t^P)_{ij} = \frac{1}{4\sqrt{2}} \sum_{k=1}^3 \frac{\lambda'_{iak} \lambda_{jbk}^*}{m_{\tilde{d}_{Rk}}^2}. \quad (12)$$

The s -channel contribution can be calculated from the interaction Lagrangian

$$\mathcal{L} = \lambda_{ijk} \left\{ -\overline{(\tilde{l}_R)_k} (\nu_L)_j (\tilde{l}_L)_i \right\} + \lambda'_{ijk} \left\{ -\overline{(d_R)_k} (u_L)_j (\tilde{l}_L)_i \right\} + \text{h.c.} \quad (13)$$

The effective Lagrangian is given by

$$\mathcal{L}_{\text{eff}}^s = -\frac{1}{4} \sum_{k=1}^3 \frac{\lambda_{kji}^* \lambda'_{kab}}{m_{\tilde{l}_{Lk}}^2} \bar{\nu}_j (1 + \gamma_5) l_i \bar{d}_b (1 - \gamma_5) u_a. \quad (14)$$

From (11) and equations of motion for u, d quarks, we find

$$\langle 0 | \bar{d}_b \gamma_5 u_a | P(q) \rangle = -i \frac{m_P^2}{m_{u_a} + m_{d_b}} f_P. \quad (15)$$

Using (15), we obtain the s -channel contribution as

$$(A_s^P)_{ij} = -\frac{1}{2\sqrt{2} m_{l_i}} \frac{m_P^2}{m_{u_a} + m_{d_b}} \sum_{k=1}^3 \frac{\lambda_{kji}^* \lambda'_{kab}}{m_{\tilde{l}_{Lk}}^2}. \quad (16)$$

The charged Higgs contribution can be calculated from the interaction Lagrangian,

$$\begin{aligned} \mathcal{L} = & V_{u_a d_b}^* \left\{ \frac{g m_{d_b}}{\sqrt{2} m_W} \tan \beta \bar{d}_b P_L u_a H^- + \frac{g m_{u_a}}{\sqrt{2} m_W} \cot \beta \bar{d}_b P_R u_a H^- \right\} \\ & + \frac{g m_{l_i}}{\sqrt{2} m_W} \tan \beta \bar{\nu}_i P_R l_i H^+ + \text{h.c.}, \end{aligned} \quad (17)$$

where g denotes the $\text{SU}(2)_L$ gauge coupling constant, and $\tan \beta \equiv \langle H_u \rangle / \langle H_d \rangle$ is a ratio of the vacuum expectation values of two Higgs doublets H_u (the weak hypercharge $Y = 1/2$) and H_d ($Y = -1/2$). We obtain the charged Higgs contribution A_s^P from (17) as

$$A_H^P = -G_F V_{u_a d_b}^* \frac{m_{d_b}}{m_{u_a} + m_{d_b}} \frac{m_P^2}{m_{H^-}^2} \left(\tan^2 \beta - \frac{m_{u_a}}{m_{d_b}} \right). \quad (18)$$

Note that since leptons in the final state due to the charged Higgs exchange are flavor diagonal, the indices i, j are suppressed in l.h.s. of (18).

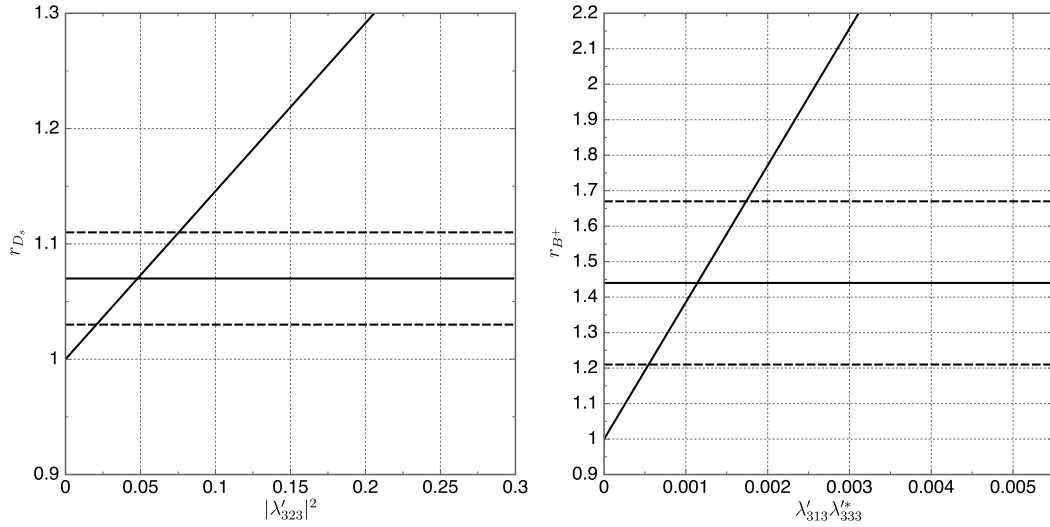


Figure 1: Contribution of t -channel squark exchange to the r -parameters (7) for $D_s \rightarrow \tau\nu_\tau$ (left) and $B^+ \rightarrow \tau\nu_\tau$ (right) as functions of the RPV couplings. The squark mass is fixed at 100 GeV. The horizontal lines denote the $1\text{-}\sigma$ constraints on r_{D_s} and r_{B^+} given in eqs. (20a) and (20b), respectively.

3 Numerical Study

Next we examine the RPV contributions to the leptonic decays $P \rightarrow \tau\nu_\tau$ ($P = D_s$ or B^+) numerically. In the numerical study, we adopt the central values of the following parameters [27]

$$\begin{aligned} |V_{cs}| &= 1.023 \pm 0.036, & |V_{ub}| &= (3.89 \pm 0.44) \times 10^{-3}, \\ m_{D_s} &= 1968.47 \pm 0.33 \text{ MeV}, & m_{B^+} &= 5279.17 \pm 0.29 \text{ MeV}, \end{aligned} \quad (19)$$

In the analysis, we drop the second term in r.h.s. of (7), i.e., the flavor off-diagonal final state such as $\tau\nu_\mu$ or $\tau\nu_e$ are neglected. Since the RPV couplings responsible for $P \rightarrow \tau\nu_\mu$ or $P \rightarrow \tau\nu_e$ induce the lepton flavor violating processes $\tau \rightarrow \mu\gamma$ or $\tau \rightarrow e\gamma$, those couplings must be highly suppressed. Therefore we neglect the $\tau\nu_\mu$ and $\tau\nu_e$ channels in the following study, i.e., $A_{ij}^P = 0$ for $i \neq j$. Throughout our study, the squark and slepton masses are fixed at 100 GeV. For simplicity, in the t -channel diagram we consider the sbottom exchange. On the other hand, the stau exchange is forbidden in the s -channel diagram, and we consider the smuon exchange. Let us recall that s -channel amplitude is proportional to a product of λ and λ' . Since the final state is $\tau\nu_\tau$, the RPV coupling λ_{i33} requires $i \neq 3$ due to the anti-symmetric property of λ_{ijk} for the first two indices. This is why the stau exchange is forbidden in the s -channel diagram in $P \rightarrow \tau\nu_\tau$.

We first study the contribution of t -channel squark exchange in $D_s \rightarrow \tau\nu_\tau$. When the sbottom exchange diagram is dominant, the contribution to the parameter r_{D_s} is given by a coupling λ'_{323} , while the parameter r_{B^+} is given by a product $\lambda'_{313}\lambda_{333}^*$. In Fig. 1, we show the sbottom contribution to r_{D_s} for $D_s \rightarrow \tau\nu_\tau$ (left) and r_{B^+} for $B^+ \rightarrow \tau\nu_\tau$ (right) as a function of $|\lambda'_{323}|^2$ and $\lambda'_{313}\lambda_{333}^*$, respectively. The horizontal lines denote constraints on r_{D_s} from (1) and (2), and r_{B^+} from (3) and (4)

$$r_{D_s} = 1.07 \pm 0.04, \quad (20a)$$

$$r_{B^+} = 1.44 \pm 0.23. \quad (20b)$$

From Fig. 1, we find that the t -channel contribution constructively interferes with the W -boson exchange, i.e., $r_{D_s}, r_{B^+} \geq 1$. Taking account of eqs.(20a) and (20b), constraints on the RPV couplings at 1- σ level are given as

$$0.02 \lesssim |\lambda'_{323}|^2 \lesssim 0.07, \quad (21)$$

$$0.0006 \lesssim \lambda'_{313}\lambda_{333}^* \lesssim 0.0017. \quad (22)$$

The allowed RPV couplings for $B^+ \rightarrow \tau\nu_\tau$ (22) is smaller than that for $D_s \rightarrow \tau\nu_\tau$ (21) by few orders of magnitude. This is because the parameter r_P (7) accounts for the relative size of new physics contribution against for a CKM matrix element. Note that the CKM matrix element in r_{B^+} is $V_{ub} \sim 10^{-3}$, while that in r_{D_s} is $V_{cs} \sim 1$. Thus, the difference of magnitude between V_{cs} and V_{ub} explains the difference between (21) and (22).

Next we study the s -channel slepton exchange. From (16), we find that the interference between the s -channel contribution and the W -boson exchange is destructive when the RPV couplings are real and positive. We show the r_{D_s} parameter via the s -channel slepton exchange, and the interference between the s - and t -channel exchanges in Fig. 2. Note that the t -channel contribution is proportional to $|\lambda'_{323}|^2$ while the s -channel contribution is $\lambda'_{222}\lambda_{233}^*$. The solid curve represents the t -channel contribution which is obtained by setting $\lambda^2 = |\lambda'_{323}|^2$ and $\lambda'_{222}\lambda_{233}^* = 0$. On the other hand, the dotted curve denotes the s -channel contribution which is obtained by setting the t -channel coupling to zero, i.e., $\lambda^2 = \lambda'_{222}\lambda_{233}^*$ and $|\lambda'_{323}|^2 = 0$. The sum of the t - and s -channel diagrams is given by the dashed curve, where we fix the RPV couplings in both t - and s -channel diagrams to be equal, $\lambda^2 = |\lambda'_{323}|^2 = \lambda'_{222}\lambda_{233}^*$ for comparison of contributions from each diagram. It is clear that, when $\lambda'_{222}\lambda_{233}^* > 0$, the s -channel slepton exchange diagram destructively interferes with both the SM W -boson and t -channel squark exchange diagrams. Therefore, the squark (t -channel) and slepton (s -channel) contributions may be cancelled each other in some parameter space. In the dashed line

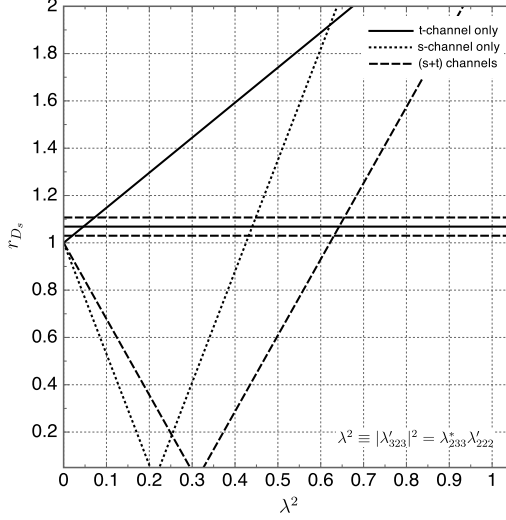


Figure 2: Contribution of RPV interactions to the parameter r_{D_s} as functions of the RPV couplings. Three curves correspond to the t -channel contribution (solid), the s -channel contribution (dotted) and the sum of s - and t -channel contributions (dashed). For comparison of contributions from each diagram, we fix the RPV couplings in both t - and s -channel diagrams to be equal, i.e., $\lambda^2 \equiv |\lambda'_{323}|^2 = \lambda'_{233} \lambda'^*_{222}$. The horizontal lines denote the $1\text{-}\sigma$ bound on r_{D_s} from the experimental data.

which represents the sum of s - and t -channel the r_{D_s} parameter decreases from unity and becomes zero (i.e., $G_F V_{cs} + A_t^{D_s} \approx -A_s^{D_s}$) around $\lambda^2 \sim 0.3$. For $\lambda^2 \gtrsim 0.3$, the s -channel contribution eventually dominates over the W -boson and t -channel squark contribution ($G_F V_{cs} + A_t^{D_s} \ll |A_s^{D_s}|$) and the r_{D_s} parameter increases with λ^2 , which satisfies the experimental constraint when $\lambda^2 \sim 0.65$. From Fig. 2 we find the relation $A_t^{D_s} < A_s^{D_s}$ holds and this can be understood as follows. When the RPV couplings and sparticle masses are same in both the t -channel contribution A_t^P (12) and the s -channel contribution A_s^P (16), the relative magnitudes of two contributions are determined by their coefficients, $\frac{1}{4\sqrt{2}}$ for the t -channel and $\frac{1}{2\sqrt{2}} \frac{m_P}{m_{l_i}} \frac{m_P}{m_{U_a} + m_{D_b}}$ for the s -channel. Note that the ratio $\frac{m_P}{m_{U_a} + m_{D_b}}$ is of order unity for $P = D_s$ or B^+ . On the other hand, the s -channel contribution A_s^P could be enhanced by the ratio $\frac{m_P}{m_{l_i}}$. For $l_i = \tau$, the ratio is $\frac{m_P}{m_\tau} \sim 1$ for $P = D_s$ and ~ 3 for $P = B^+$. Therefore, the size of A_s^P is about 2(8) times larger than A_t^P for $D_s(B^+)$ when the RPV couplings and the sparticle masses are common. It should be mentioned that the s -channel contribution $A_s^{D_s}$ is considerably larger for $l = \mu(e)$ than for $l = \tau$ due to small lepton mass.

In Fig. 3, we show constraints on the RPV couplings from $D_s \rightarrow \tau \nu_\tau$ (left) and $B^+ \rightarrow \tau \nu_\tau$ (right). The horizontal axis represents the RPV couplings for t -channel

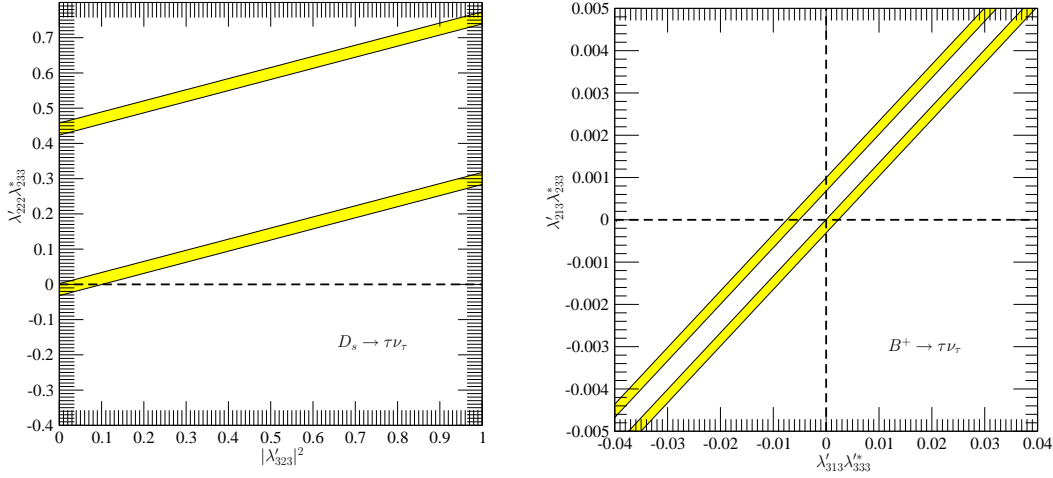


Figure 3: Constraints on the RPV couplings from $D_s \rightarrow \tau \nu_\tau$ (left) and $B^+ \rightarrow \tau \nu_\tau$ (right). The horizontal axis represents the RPV couplings for t -channel while the vertical axis denotes the couplings for s -channel. The bands with solid line correspond to the 2- σ allowed range for the r_{D_s} (left) and r_{B^+} (right) parameters, respectively. In each figure, the inner lines correspond to the 2- σ lower bounds while the outer are the 2- σ upper bounds on r_{D_s} and r_{B^+} , respectively.

diagram while the vertical axis denotes the couplings for s -channel diagram. The bands with solid lines correspond to the 2- σ allowed range for r_{D_s} (20a) and r_{B^+} (20b). In each figure, the inner solid lines correspond to the 2- σ lower bounds while the outer are the 2- σ upper bounds on r_{D_s} and r_{B^+} , respectively. From Fig. 3, we find that the s -channel couplings have positive correlations with the t -channel couplings. This is because the interference between the s - and t -channel contributions is destructive. For $D_s \rightarrow \tau \nu_\tau$, since the t -channel coupling is always positive ($|\lambda'_{323}|^2 \geq 0$), not only the magnitude but also the sign of s -channel coupling $\lambda'_{222}\lambda_{233}^*$ is strongly constrained. For negative $\lambda'_{222}\lambda_{233}^*$, the t -channel coupling $|\lambda'_{323}|^2$ should be smaller than 0.12 and, then, $-0.04 \lesssim \lambda'_{222}\lambda_{233}^* \leq 0$ is experimentally allowed in the 2- σ level. For $B^+ \rightarrow \tau \nu_\tau$, the s - and t -channel couplings with opposite signs are strongly constrained. As can be seen in Fig. 3, when the t -channel coupling is positive ($\lambda'_{313}\lambda_{333}^* \geq 0$), the negative s -channel coupling is constrained to be $-0.0004 \lesssim \lambda'_{213}\lambda_{233}^* \leq 0$. Although the leptonic decays of D_s and B^+ mesons are useful to constrain the sign of the relevant RPV couplings, the size of the couplings cannot be restricted because of the cancellation among the diagrams. However, the correlations among the RPV couplings as shown in Fig. 3 may be a good information to test the R -parity violating SUSY-SM at the direct search experiments such as LHC, because some RPV couplings could be large simultaneously

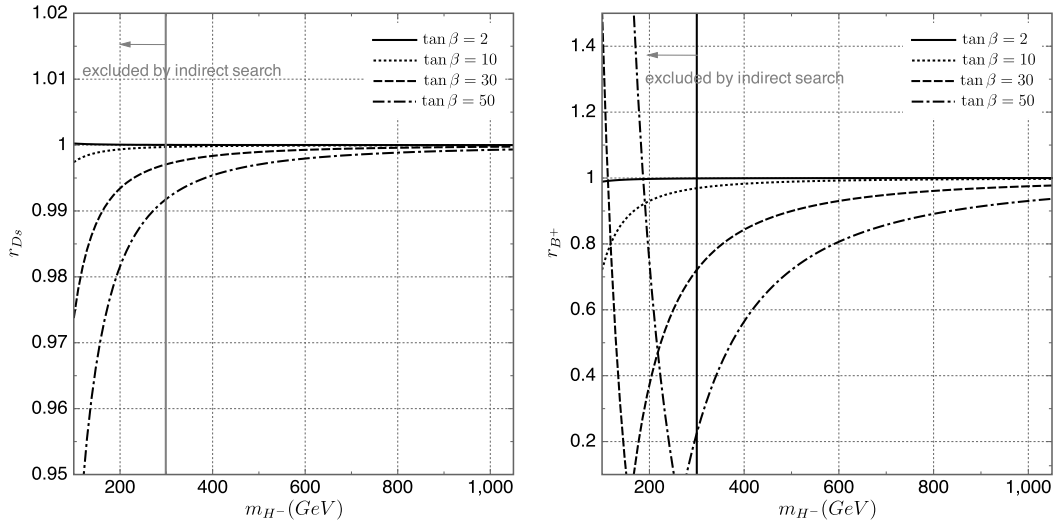


Figure 4: The charged Higgs contributions to r_{D_s} (left) and r_{B^+} (right) as functions of the charged Higgs boson mass m_{H^-} . The four curves (solid, dotted, dashed and dot-dashed) correspond to $\tan\beta = 2, 10, 30$ and 50 , respectively. The vertical line denotes the lower bound on $m_{H^-} > 295\text{GeV}$ from the $b \rightarrow s\gamma$ decay [28].

and it may lead to observation of several productions or decay processes due to the RPV interactions.

In the MSSM with RPV couplings, in addition to the contributions via squark and slepton exchanges, the charged Higgs boson H^- also affect the leptonic decay of a pseudo scalar meson through the s -channel diagram. We show the charged Higgs contributions to r_{D_s} and r_{B^+} as functions of the mass m_{H^-} in Fig. 4. In each figure, four curves are obtained for $\tan\beta = 2, 10, 30$ and 50 . The vertical line denotes the lower bound on the mass of charged Higgs boson from the experimental data of $b \rightarrow s\gamma$, $m_{H^-} > 295\text{ GeV}$ [28]². It is easy to see that the charged Higgs contribution to $D_s \rightarrow \tau\nu_\tau$ is marginal (smaller than 1%) for $m_{H^-} > 295\text{ GeV}$. On the other hand, the contribution to $B^+ \rightarrow \tau\nu_\tau$ could be as large as 80% for $\tan\beta = 50$. However, it destructively interferes with the W -boson exchange so that the charged Higgs contribution is disfavored from the current experimental data of $B^+ \rightarrow \tau\nu_\tau$. Thus, the charged Higgs contribution cannot explain the deviation between the data and the SM prediction in the leptonic decay of B^+ meson. Comparison of constraints on the RPV couplings from $B^+ \rightarrow \tau\nu_\tau$ with and without the charged Higgs exchange is shown in Fig. 5. The bands with solid

² This constraint has been obtained on Type-II two Higgs doublet model (THDM-II). Although the Higgs sector in the MSSM has the same structure with THDM-II, the contributions of H^- to $b \rightarrow s\gamma$ could be canceled with those from charginos. Therefore, the constraint on m_{H^-} which we adopted here corresponds to the decoupling limit of chargino so that it may be conservative.

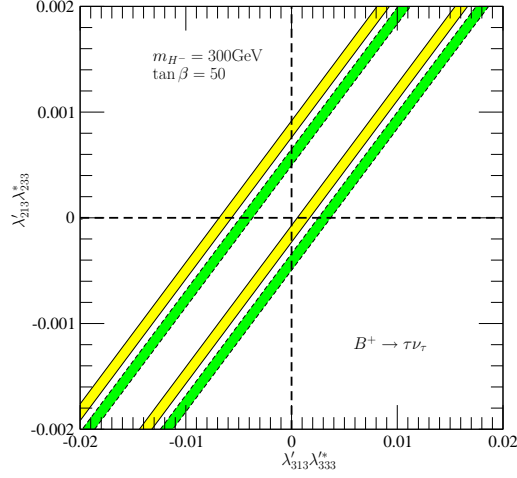


Figure 5: Constraints on the RPV couplings from $B^+ \rightarrow \tau \nu_\tau$. The bands with solid and dotted lines correspond to the $1\text{-}\sigma$ allowed range for the r_{B^+} parameter with and without the contribution from charged Higgs exchange, respectively. The contribution of charged Higgs boson is estimated for $m_{H^-} = 300$ GeV and $\tan \beta = 50$.

and dotted lines correspond to the $1\text{-}\sigma$ allowed range for r_{B^+} with and without the charged Higgs exchange, respectively. The contribution of charged Higgs exchange is estimated for $m_{H^-} = 300$ GeV and $\tan \beta = 50$, which is a parameter set to give most sizable contribution to $B^+ \rightarrow \tau \nu_\tau$ under the experimental constraints from $b \rightarrow s \gamma$ as shown in Fig. 4. The contribution of charged Higgs boson slightly alters the allowed region of the RPV couplings. For example, when the s -channel RPV couplings are zero ($\lambda'_{213} \lambda_{233}^* = 0$), the allowed range of RPV couplings with the charged Higgs contribution shifts about factor two or three from that without charged Higgs boson.

4 Summary

We have investigated the leptonic decays of D_s and B^+ mesons in R -parity violating supersymmetric SM. The experimental data of leptonic decays $D_s \rightarrow \tau \nu_\tau$ and $B^+ \rightarrow \tau \nu_\tau$ show about 2.4 and $2.5\text{-}\sigma$ deviations from the SM (Lattice QCD) predictions. We found the parameter space of the R -parity violating supersymmetric SM to explain the above deviations. It was shown that the interference between the s -channel slepton exchange and t -channel squark exchange diagrams could be either constructive or destructive, owing to a choice of relative sign between the RPV couplings in two diagrams. We also found that when the relative sign of the RPV couplings between the s - and t -channels is opposite, the allowed parameter region is strongly restricted from the experimental

data. For example, in case of $D_s \rightarrow \tau \nu_\tau$, the negative s -channel coupling $\lambda'_{222} \lambda_{233}^* \leq 0$ is allowed only when the t -channel coupling is $|\lambda'_{323}|^2 \lesssim 0.012$. In case of $B^+ \rightarrow \tau \nu_\tau$, the RPV couplings $\lambda'_{213} \lambda_{233}^* < 0$ in s -channel and $\lambda'_{313} \lambda_{333}^* > 0$ in t -channel are constrained to be less than 10^{-3} . The charged Higgs contribution always destructively interferes with the SM W -boson contribution. Taking account of constraints on the charged Higgs mass from the $b \rightarrow s \gamma$ decay, we found that the charged Higgs contribution to the parameter r_{D_s} is marginal while that to r_{B^+} could be sizable for large $\tan \beta$ because of the enhancement of the bottom-Yukawa coupling. We presented how the constraints on RPV couplings are altered with and without charged Higgs contribution in $B^+ \rightarrow \tau \nu_\tau$.

A distinct feature of our work from the previous studies is that the RPV couplings related to $D_s \rightarrow \tau \nu_\tau$ and $B^+ \rightarrow \tau \nu_\tau$ could be sizable *simultaneously* due to the positive correlation between the s - and t -channel diagrams. Since the expected sensitivity of the RPV couplings at LHC is, e.g., $0.1 - 0.01$ for λ'_{ijk} from the single sparticle production events with the integrated luminosity $\int dt \mathcal{L} = 30 \text{fb}^{-1}$ [22], the allowed parameter space of the RPV couplings which is found in our study will be covered and our scenario to explain the deviation in the leptonic decays of D_s and B^+ mesons using the RPV couplings could be tested.

References

- [1] For a review, see: S. P. Martin, arXiv:hep-ph/9709356.
- [2] L. J. Hall and M. Suzuki, Nucl. Phys. B **231**, 419 (1984).
- [3] W. Buchmuller, L. Covi, K. Hamaguchi, A. Ibarra and T. Yanagida, JHEP **0703**, 037 (2007) [arXiv:hep-ph/0702184].
- [4] P. Naik *et al.* [The CLEO Collaboration], Phys. Rev. D **80**, 112004 (2009) [arXiv:0910.3602 [hep-ex]].
- [5] E. Follana, C. T. H. Davies, G. P. Lepage and J. Shigemitsu [HPQCD Collaboration and UKQCD Collaboration], Phys. Rev. Lett. **100**, 062002 (2008) [arXiv:0706.1726 [hep-lat]].
- [6] A. S. Kronfeld, arXiv:0912.0543 [hep-ph]; A. A. Petrov, arXiv:1003.0906 [hep-ph].
- [7] K. Ikado *et al.* [Belle Collaboration], Phys. Rev. Lett. **97**, 251802 (2006) [arXiv:hep-ex/0604018];

- [8] B. Aubert *et al.* [BABAR Collaboration], Phys. Rev. D **77**, 011107 (2008) [arXiv:0708.2260 [hep-ex]]; B. Aubert *et al.* [BABAR Collaboration], Phys. Rev. D **81**, 051101 (2010) [arXiv:0809.4027 [hep-ex]]; I. Adachi *et al.* [Belle Collaboration], arXiv:0809.3834 [hep-ex];
- [9] M. Bona *et al.* [UTfit Collaboration], Phys. Lett. B **687**, 61 (2010) [arXiv:0908.3470 [hep-ph]].
- [10] G. Burdman, J. T. Goldman and D. Wyler, Phys. Rev. D **51**, 111 (1995) [arXiv:hep-ph/9405425].
- [11] Y. H. Ahn and C. H. Chen, Phys. Lett. B **690**, 57 (2010) [arXiv:1002.4216 [hep-ph]].
- [12] A. G. Akeroyd and F. Mahmoudi, JHEP **0904**, 121 (2009) [arXiv:0902.2393 [hep-ph]].
- [13] A. G. Akeroyd and C. H. Chen, Phys. Rev. D **75**, 075004 (2007) [arXiv:hep-ph/0701078].
- [14] B. A. Dobrescu and A. S. Kronfeld, Phys. Rev. Lett. **100**, 241802 (2008) [arXiv:0803.0512 [hep-ph]].
- [15] R. Benbrik and C. H. Chen, Phys. Lett. B **672**, 172 (2009) [arXiv:0807.2373 [hep-ph]].
- [16] S. Baek and Y. G. Kim, Phys. Rev. D **60**, 077701 (1999) [arXiv:hep-ph/9906385];
- [17] H. K. Dreiner, G. Polesello and M. Thormeier, Phys. Rev. D **65**, 115006 (2002) [arXiv:hep-ph/0112228].
- [18] H. K. Dreiner, M. Kramer and B. O'Leary, Phys. Rev. D **75**, 114016 (2007) [arXiv:hep-ph/0612278].
- [19] A. Kundu and S. Nandi, Phys. Rev. D **78**, 015009 (2008) [arXiv:0803.1898 [hep-ph]].
- [20] Y. Kao and T. Takeuchi, arXiv:0909.0042 [hep-ph].
- [21] G. Bhattacharyya, K. B. Chatterjee and S. Nandi, Nucl. Phys. B **831**, 344 (2010) [arXiv:0911.3811 [hep-ph]].
- [22] R. Barbier *et al.*, Phys. Rept. **420**, 1 (2005) [arXiv:hep-ph/0406039].

- [23] V. D. Barger, G. F. Giudice and T. Han, Phys. Rev. D **40**, 2987 (1989).
- [24] H. K. Dreiner, in 'Perspectives on Supersymmetry', Ed. by G.L. Kane, World Scientific, p462-479 [arXiv:hep-ph/9707435].
- [25] G. Bhattacharyya, Talk given at Workshop on Physics Beyond the Standard Model: Beyond the Desert: Accelerator and Nonaccelerator Approaches, Tegernsee, Germany, 8-14 Jun 1997 [arXiv:hep-ph/9709395].
- [26] B. C. Allanach, A. Dedes and H. K. Dreiner, Phys. Rev. D **60**, 075014 (1999) [arXiv:hep-ph/9906209].
- [27] K. Nakamura et al. (Particle Data Group), J. Phys. G **37**, 075021 (2010)
- [28] M. Misiak *et al.*, Phys. Rev. Lett. **98**, 022002 (2007) [arXiv:hep-ph/0609232].